

## Numerical Analysis of Gas-Solid Behavior in a Cyclone Separator for Circulating Fluidized Bed System

Prabhansu<sup>1†</sup>, S. Rajmistry<sup>1</sup>, S. Ganguli<sup>2</sup>, P. Chandra<sup>1</sup>, M. Kr karmakar<sup>2</sup> and P. Kr Chatterjee<sup>2</sup>

<sup>1</sup>*Department of Mechanical Engineering, National Institute of Technology Patna-800005, India*

<sup>2</sup>*Energy Research and Technology, CSIR-Central Mechanical Engineering Research Institute, Durgapur-713209, India*

†Corresponding author Email: [prabhansu.me13@nitp.ac.in](mailto:prabhansu.me13@nitp.ac.in)

(Received July 19, 2016; accepted February 16, 2017)

### ABSTRACT

Cyclones are one of the most widely used gas-solid separators in circulating fluidized bed (CFB) systems. This paper focuses on numerical study of the gas-solid flow in a cyclone attached to the CFB system. The objective was to understand the flow pattern in the cyclone in order to run the CFB setup problem free. The previous works on cyclone separators do not include critical parameter such as coefficient of restitution which is responsible for swirling effect and increase in efficiency. Reynolds stress model (RSM) is used to obtain the gas flow characteristics. The resulting flow and pressure fields are verified by comparing with the measured experimental results and then used in the determination of solids flow that is simulated by the use of a discrete phase model. The simulation results show how the particle trajectories and cyclone efficiency change with varying coefficient of restitution and particle size keeping inlet velocity of gas and mean particle diameter constant. The separation efficiency, pressure drop and particle trapping time from the numerical analysis are shown to be comparable to those observed experimentally. The velocity distribution pattern obtained from the analysis exhibits strong flow recirculation with large turbulent eddies in the cyclone separator. The particle trajectories depend upon relative velocity of fluid/particles and concentration of particles. Efficiency of the cyclone is found to be dependent on particle size and coefficient of restitution. The results obtained are further utilized to optimize the velocity range of gas flow in the loop seal and riser for stable operation of CFB setup.

**Keywords:** Cyclone; Reynolds stress model; Coefficient of restitution; Circulating fluidized bed.

### NOMENCLATURE

$C_D$	drag coefficient	$u_p$	particle instantaneous velocity in axial direction
$d$	particle diameter	$v$	time average velocity in radial direction
$F_k$	momentum transport coefficient	$v_p$	particle instantaneous velocity in radial direction
$g$	acceleration due to gravity	$w$	time average velocity in tangential direction
$g$	gas	$w_p$	particle instantaneous velocity in tangential direction
$i, j, k$	1,2,3	$x$	axis
$p'$	dispersion pressure	$\delta$	kronecker factor
$p$	particle	$\mu$	fluid viscosity
$Re$	Reynolds number	$\rho$	density
$r_p$	radius of particle		
$t$	time		
$u$	instantaneous velocity		
$\bar{u}$	time average velocity in axial direction		
$u'$	dispersion velocity		

### 1. INTRODUCTION

In circulating fluidized bed (CFB) reactors,

cyclones are integrated into the external solid loop to recycle and separate the entrained solids in a mixture of gas-solid from reactor by

gravitational and rotational effect. In a typical cyclone as suggested by Bloor *et al.* (1957), Bloor *et al.* (1975), Slack *et al.* (2000), and Fraser *et al.* (2000), the mixture enters the inlet of the cyclone tangentially and accelerates in a helical pattern on its way down into conical section resulting in complex flow pattern with strong swirling motion. Heavier particles in the mixture have too much inertia to follow the stream curve, hence they strike the outside wall and then slide down to the bottom of cyclone, where they are collected and sent back to the riser through downcomer of the CFB reactor, while the very fine particles reverse and swirl along the center line and get escaped from the cyclone through vortex finder. Previous work has been done by Leith *et al.* (1973) to predict cyclone pressure drop and efficiency in the past. Conventionally prediction of the flow field and the separation efficiency of cyclone separator were empirical. Over the last few decades, computational fluid dynamics (CFD) is being widely used for the numerical study and calculation of gas flow field in a cyclone. Boysan *et al.* (1982) performed computational simulations and found the inadequacy in the standard  $k-\epsilon$  turbulence model for flows with swirl as it ends up in highly unrealistic tangential velocities and turbulence viscosities. Studies by Hoekstra *et al.* (1999), Pant *et al.* (2002) and Sommerfeld *et al.* (2003) suggests that Reynolds Stress Model (RSM) is best suited for numerical solution of cyclones. Particles can be taken as second phase and to simulate them Discrete Phase Model (DPM) can be used.

Some of Recent works conducted for cyclone simulation includes Chengming Song *et al.* (2016), where Reynolds stress model (RSM) and stochastic Lagrangian particle tracking model (LPT) were used to simulate the turbulent flow of gas. Design modification in the cyclone has been reported by Hamed Safikhani *et al.* (2016) where an outer cylinder and a vortex limiter replaced the separation space of conventional cyclone. Operational conditions and particle properties on deposition was investigated by Jianfei Song *et al.* (2017) for 500 mm-diameter cyclone where the distribution range and size of deposited particles was found similar to that in industrial cyclones. Another work by Marek Wasilewski *et al.* (2017) introduced additional compartment in the form of a counter-cone in order to optimize the structure of cyclone separators where 15 variants were tested. In another work by Osama Hamdya *et al.* (2017), six different cyclone separator designs were tested numerically to analyze the effect of gas flow field by changing cone length. High particle loads were analyzed by Paweł Kozolub *et al.* (2016) using a numerical simulation of the flow inside a cyclone separator. Sakura Ganegama Bogodage *et al.* (2015) presented CFD modelling of gas–solid

flow in cyclone separators having different dust outlet geometries for cases with and without downcomer tubes at the cyclone bottom and examined the flow characteristics and the cyclone performance. Convergent cyclone separator were used by Seyed Ehsan Rafiee *et al.* (2017) for the analysis on separation phenomenon influenced by the structural factors like throttle angle, non-dimensional throttle diameter, convergence main tube angle, non-dimensional convergent length, injector slots number and injection pressure. The pressure and flow field in high efficiency cyclone separator were investigated by J.J.H. Houben *et al.* (2016). In these simulations, the position of the vortex core were tracked and searched for the locations of minimal dynamic pressure and for the centre of moment of the horizontal velocity components as a function of the axial coordinate. An experimental and numerical simulation was presented for cyclone separator by K. Talbi *et al.* (2011) concerning the 3-D turbulent flow of air underneath the vortex finder. Laser Doppler Anemometry was used to measure the axial and tangential mean velocity components and the turbulence intensities for the study.

In the current work, RSM and DPM models of ANSYS Fluent 15.0 are used to analyze the gas-solid flow in a typical Lapple cyclone separator. To verify the simulation results, comparison was done with the measured results in term of pressure drop, flow fields, solid flow pattern and separation efficiency. The effects of particle size and coefficient of restitution on separation efficiency and pressure drop of cyclone with the change in velocities are discussed.

## 2. EXPERIMENTAL SETUP

The cyclone used for the computational analysis is replica of the one, which is an integral part of circulating fluidized bed (CFB) system installed at CSIR-CMERI Durgapur, India. The pictorial and schematic view of the cyclone in the CFB setup is shown in Fig. 1a and Fig. 1b and is made of stainless steel. During hydrodynamics study of this system, it was found that the circulation loop was often disturbed and the back flow of particles occurred through the cyclone, resulting in huge loss of particles. It was important for the team to have clear picture of the characteristics of cyclone in order to have better understanding of the existing CFB setup. To serve this objective, a series of experiments were conducted at atmospheric conditions on this system. Some parts of it were made Perspex glass for proper visualization of particles. There are two pressure taps (for the measurement of drop in pressure) located, one at the entry i.e., P4 and the other at the exit of cyclone i.e., P6. Common silica sand was selected for the study as it is readily available

and its density is comparable to coal. Three different sand samples were prepared using standard sieves and their properties are presented in Table 1. Compressed air was used for maintaining proper circulation of sand, supplied through air compressor line to the riser and loop seal distributor plates.



Fig. 1a. Pictorial view of CFB setup.

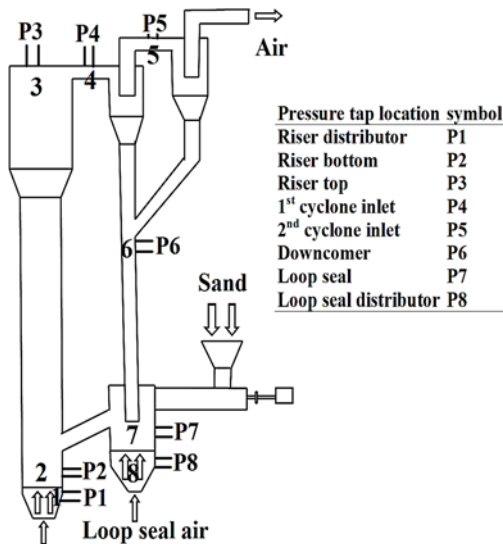


Fig. 1b. Schematic diagram of cyclone in the CFB setup.

Mass of the sand samples was kept constant at 6 kg in all the cases. For the sake of proper sight of movement of these samples, some sand (fixed quantity of weight) were blackened (mixed with coal dust) to distinguish them from the bulk sand. With the help of stop watch, time taken by the blackened sand, to

move from inlet of cyclone (riser top of the CFB) to the exit of the cyclone (downcomer of the CFB), was recorded. U-tube water manometer was used to measure the pressure drop across the cyclone. The loss of material from the system was collected for a particular run time and was weighed to calculate the experimental separation efficiency of cyclone. As the material of cyclone is stainless steel and there was no pressure tap inside the cyclone, so it was difficult to understand the phenomena occurring in that region. For that numerical modeling and CFD analysis was done and results were compared for total residence time, separation efficiency and pressure drop with the obtained experimental results.

Table 1 Properties of used sand sample

Property	Sand I	Sand II	Sand III
Size range ( $\mu\text{m}$ )	100-425	200-600	300-1000
Sauter mean diameter ( $\mu\text{m}$ )	314	414	520
Sphericity	0.86	0.86	0.86
Particle density ( $\text{kg}/\text{m}^3$ )	2500	2500	2500
Bulk density ( $\text{kg}/\text{m}^3$ )	1410	1417	1447

### 3. MATHEMATICAL MODEL

Generally three models are employed in cyclone simulation: algebraic stress model (ASM),  $k-\epsilon$  model and RSM. According to Hoekstra *et al.* (1999), ASM belittles the effect of stress convection; hence it is unable to completely predict the Rankine vortex and circulation zone in strong swirling flow. The  $k-\epsilon$  model takes assumption of isotropic turbulence in the flow field, so it is inappropriate as the flow has anisotropic turbulence in the cyclone. RSM considers anisotropic turbulence and solves transport equation for each component of Reynolds stress, hence it is accepted as the most applicable turbulence model for cyclone flow field. According to Pant *et al.* (2002) and Sommerfeld *et al.* (2003), the only disadvantage of this model is being more computationally expensive compare to other unresolved-eddy turbulence models.

In RSM, Shun and Li (2002) shown that the transport equation is written as:

$$\frac{\partial(\rho \overline{u_i u_j})}{\partial t} + \frac{\partial(\rho u_k \overline{u_i u_j})}{\partial x_k} = D_{ij} + P_{ij} + \Pi_{ij} - \epsilon_{ij} + S \quad (1)$$

Where, the left two terms are the local time derivative of stress and convective transport term, respectively. The right side terms are:

Geometrical Description	
D	Cyclone body diameter=100 mm
Ls	Cyclone barrel length =200 mm
Zc	Cyclone cone length =200 mm
b	Inlet duct height =75 mm
a	Inlet duct width =20 mm
De	Vortex finder diameter =50 mm
B	Solid educator diameter =30 mm
S	Vortex finder extension =100 mm

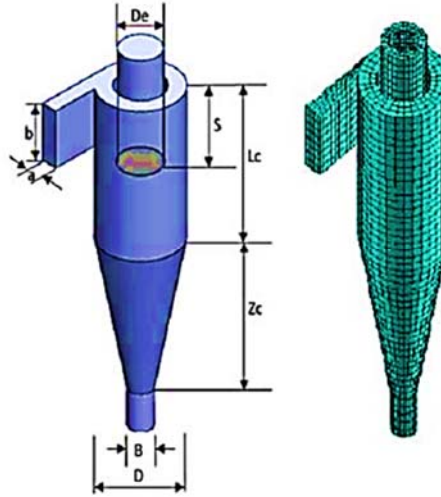


Fig. 2. Schematic representation of geometry and computational mesh for cyclone.

The stress diffusion term:

$$D_{ij} = -\frac{\partial}{\partial x_k} [\rho \overline{u'_i u'_j u'_k} + (\overline{p' u'_j}) \delta_{ik} + (\overline{p' u'_i}) \delta_{jk} - \mu \overline{\frac{\partial u'_i u'_j}{\partial x_k}}] \quad (1a)$$

The shear production term:

$$P_{ij} = -\rho [\overline{u'_i u'_k} \frac{\partial u_j}{\partial x_k} + \overline{u'_j u'_k} \frac{\partial u_i}{\partial x_k}] \quad (1b)$$

The pressure- strain term:

$$\Pi_{ij} = \overline{p' (\frac{\partial u'_i}{\partial x_j} + \frac{\partial u'_j}{\partial x_i})} \quad (1c)$$

The dissipation term:

$$\varepsilon_{ij} = -2\mu \overline{\frac{\partial u'_i}{\partial x_k} + \frac{\partial u'_j}{\partial x_k}} \quad (1d)$$

And the source term: S

In the modeling of particle dispersion, RSM model considers dilute phase, hence the interactions between particles are neglected. The Saffman force, Basset force, virtual mass force and Magnus force has not been taken into consideration. The gas drag force is composed of drag force caused by dispersion velocity and average velocity of fluid. The momentum equation of particle in the two phase flow at ambient temperature can be described by Shun and Li (2002):

$$\frac{du_p}{dt} = F_k (\bar{u} + u' - u_p) - g \quad (2)$$

$$\frac{dv_p}{dt} = F_k (\bar{v} + v - v_p) + \frac{w_p^2}{r_p} \quad (3)$$

$$\frac{dw_p}{dt} = F_k (\bar{w} + w' - w_p^2) - \frac{v_p w_p}{r_p} \quad (4)$$

Where  $F_k = \frac{18\mu}{d_p^2 \rho_p} C_D \frac{Re_p}{24}$  is the momentum transport coefficient between fluid and particles, and the drag coefficient is given as:

$$C_D = \frac{24}{Re} \quad Re_p \leq 1 \quad (5a)$$

$$C_D = \frac{24(1+0.15Re_p^{0.687})}{Re_p} \quad 1 < Re_p \leq 1000 \quad (5b)$$

$$C_D = 0.44 \quad Re_p > 1000 \quad (5c)$$

Where  $Re_p = \frac{d_p \rho_g |\overline{q_g} - \overline{q_p}|}{\mu}$  is the Particle Reynolds number. When the particle interacts with fluid eddy,  $u'$ ,  $v'$ ,  $w'$  is obtained by sampling from an isotropic Gaussian distribution with a standard deviation of  $\sqrt{\frac{2k}{3}}$ . Particle-eddy interaction time and dimension should not be larger than the size and lifetime of a random eddy.

Tangential and normal coefficient of restitution are written as

$$e_t = \frac{V_{2t}}{V_{1t}} = 1.0 - 2.12\beta_1 + 3.0775\beta_1^2 - 1.1\beta_1^3 \quad (6)$$

$$e_n = \frac{V_{2n}}{V_{1n}} = 1.0 - 0.4159\beta_1 + 4.994\beta_1^2 - 0.292\beta_1^3 \quad (7)$$

Where,  $e_t$  &  $e_n$  are the coefficients ratios, of impact velocities in tangential and normal directions.  $V_1$  &  $V_2$  are impact velocity before and after impact from the surface and  $\beta$  is the impact angle as described by Du and Tabakoff (1984) & Bhasker (2010).

#### 4. SIMULATION CONDITION

Several unstructured and structured grids were generated and tested but finally three meshes were found optimum as per computational time and cost. Total elements in three different cases of generated mesh of cyclone were 27134, 48310 and 81231. The test was initially done for 2.0 sec flow time for each mesh and it was found that the variation in results for separation efficiency and pressure drop was within 11%; hence the second mesh was selected for the analysis. Fig. 2 shows the geometrical description of cyclone and

**Table 2 Time taken by three different sand samples to get trapped experimentally and numerically**

Sand samples	Sand I		Sand II		Sand III	
	Experimental	Numerical	Experimental	Numerical	Experimental	Numerical
Travel time (in sec)	9.5	8.5	7.1	6.2	6.2	5.4

computational domain, containing 48,310 total elements. The whole computational domain is divided by multi-block structured hexahedron grids. At the zone near wall and vortex finder the grids are dense, while at the zone away from wall the grids are made sparse.

The properties of sand used for the simulation is presented in Table 1. Reynolds stress model is chosen under viscous model because of complex flow field with standard wall function. Air is chosen as the first material with fluid cell zone condition. Discrete phase model (DPM) is employed to simulate spherical solid particles as a second phase in the cyclone. So DPM is activated and tracking parameters are specified. Turbulence model is used to feed momentum, where hydraulic diameter of cyclone inlet and vortex finder is given with inlet velocity of air. Until and unless specified, velocity of inlet mixture is 14 m/s. Surface injection is created from cyclone inlet using Rosin-Rammler diameter distribution with spread parameter = 3.5 assuming particles to have same inlet velocity and incoming air. Hybrid initialization method was used to initialize the solution and after that calculation was started. Calculation run was allowed till the residuals for continuity equation are sent below  $1e-04$ . Boundary condition are set in such a way that particles should be reflected from the wall and they can escape from the vortex finder outlet and inlet of cyclone. All particles which separate from the carrier gas due to centrifugal forces and sink towards the outlet of cyclone and are reported as trapped. Particles can be tracked along with displaying trajectories of different diameter particles under graphics and animation setup and efficiency of cyclone is calculated. One time injection of 400 particles was created at the inlet of the cyclone to understand particle position clearly in the flow field and motion was hence tracked till the trap of almost all particles. Sand is used as the material for testing cyclone efficiency in the practical setup as well as in simulation. There are some particles which behave like stuck in an infinite loop and are treated as incomplete. They move up and down, never reaching the outlet of cyclone.

## 5. RESULTS AND DISCUSSION

It was found from the simulation results that

particles rotate in conical part for longer time as compared to barrel because there is frequent collision of particles with the wall of cyclone, so gravitational force does not get much time to show its effect. It is noticed that all the particles of three samples reaches the conical part of cyclone in less than 0.6 seconds.

Simulation was allowed to run for the time when almost all particles are trapped. This flow time was compared for time taken by the blackened sand to travel from inlet to outlet of cyclone and the results are presented in Table 2. It describes the total time taken by different sand samples to get trapped. It is clear from the table that larger the particle size less is the time taken to get trapped. Sand III has the largest diameter, hence it took least time to reach solid educator. The error obtained in the results is due to the inter particle, sand-wall friction, Saffman force, Basset force, virtual mass force and Magnus force which has not been considered in the numerical analysis. Deviation of numerical values from the experimental values is 10.5% for sand I, 12.7% for sand II and 12.9% sand III.

Fig. 3a, 3b and 3c shows the trajectories of different sand samples for coefficient of restitution 1, 0.9, 0.85 and 0.8. These four coefficients of restitution are considered for each sand sample. Different sand samples under consideration are tested for their efficiency and pressure drop. For constant inlet velocity, it was found that pressure drop is almost same in all the cases. The cyclone separation efficiency show drastic variation as coefficient of restitution was decreased from 1 to 0.8. For all the three sand samples, efficiency is zero if coefficient of restitution is considered to be equal to 1 and trend is same for 0.9 as most of the particles either escaped through inlet or pressure outlet and rest of them are incomplete or not trapped. At 0.85 coefficient of restitution, 100% efficiency was attained, but it has quite large number of incomplete particles which means although efficiency has reached 100% but all the particles are not trapped, which implies the loss of sand. When coefficient of restitution was further reduced to 0.8, efficiency was found to be 100% and no particle as incomplete.

Generally, large particles are collected in the outlet while small particles escape from vortex finder. The particles with the smallest

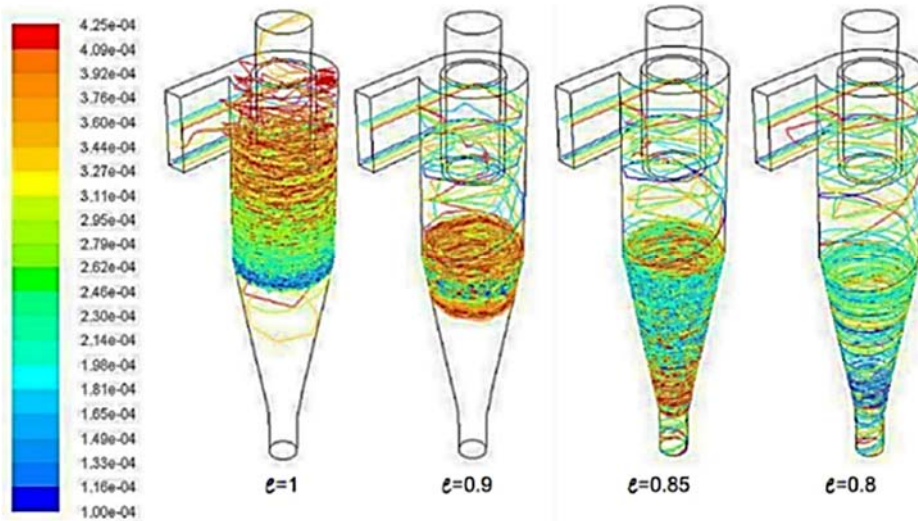


Fig. 3a. Velocity (m/s) trajectories of particles with different diameters at different coefficient of restitution for sand I.

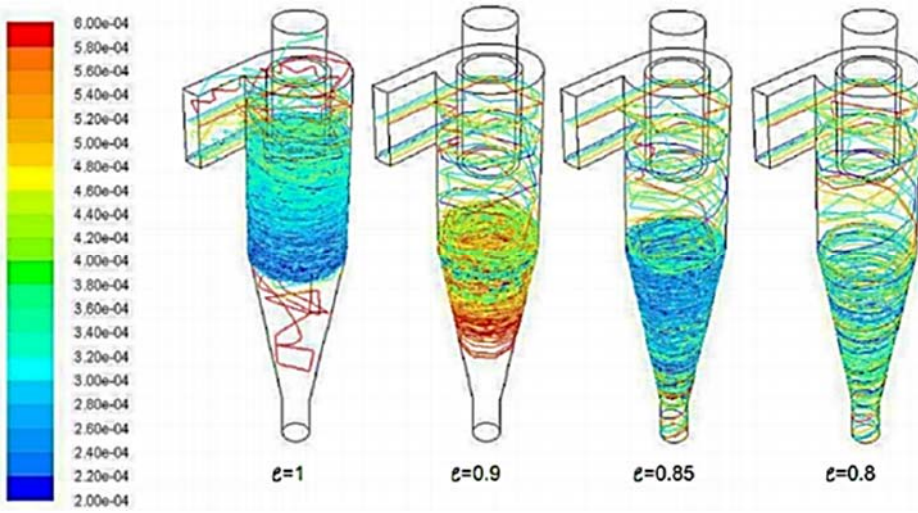


Fig. 3b. Velocity (m/s) trajectories of particles with different diameters at different coefficient of restitution for sand II.

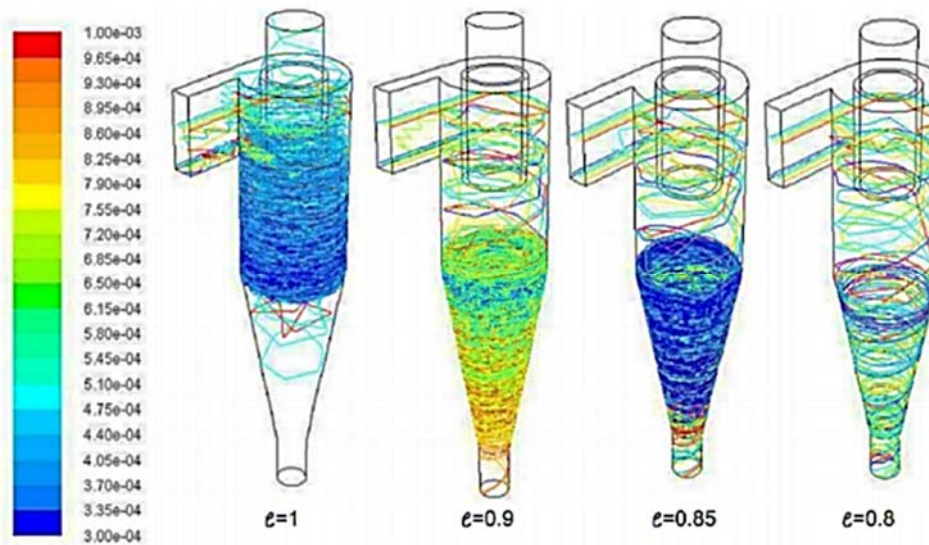


Fig. 3c. Velocity (m/s) trajectories of particles with different diameters at different coefficient of restitution for sand III.

diameter cannot move outward to the wall of cyclone since the centrifugal force on them is not bigger than the gas drag force on them. But in this study the size of particles do not vary much and all of them have size more than 100micron, so most of them settle down to outlet. Once the particle reaches a flux element boundary, a test is performed to determine the type of flux element the particle is about to enter. If the flux element is open to fluid flow, then the local grid coordinates are reset and tracking continues in the next element. If the flux element is a boundary node, then the particle has encountered boundary condition regions like wall, inlet and outlet. As investigated by Bhasker (2010), for each boundary condition, except the wall, there is only one possible particle action that the particle may escape from an inlet or an outlet. When the particles react at the wall, its remaining mass, momentum and energy is transferred to fluid. The velocity of rebounding is calculated using coefficient of restitution when the particle reacts/rebounds from the wall. The method to determine coefficient of restitution experimentally was done according to particle velocity, flow and target material by F. Jianren *et al.* (1984) and J. Y. Du *et al.* (1998). Industrial stainless steel (410) has coefficient of restitution ranging from 0.7 to 0.8 for inert sand particles so, the obtained result of 0.8 is fairly good. The flow field in cyclone shows the expected forced/free combination of the Rankine vortex.

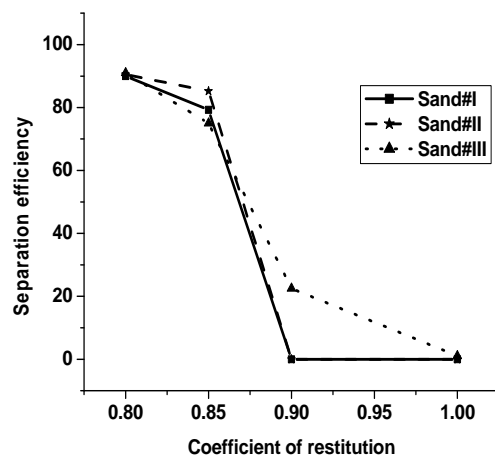


Fig. 4. Variation of separation efficiency with coefficient of restitution at 14 m/s.

As the range of particles for the three samples is almost same, so the pressure drop across the cyclone is almost constant for all the three samples. It was found that all types of sand have zero particles trapping at coefficient of restitution equals to one. As coefficient of restitution starts decreasing, number of trapped particles increases. Sand

III has best behavior for all coefficients of restitutions, hence it can be concluded that heavy particles perform well in the cyclone flow field. Fig. 4. shows the effect of coefficient of restitution on separation efficiency for different sand samples.

Figure 5a shows the contour plots for static pressure (in gauge scale) of sand sample#I which is largest near the wall of cyclone and it decreases radially from the wall to the center. There is negative pressure zone at the center. Magnitude of negative pressure in the free vortex zone of cyclone barrel is more than that in free vortex zone of vortex finder. Pressure gradient is largest along radial direction because of highly intensified forced vortex. Fig. 5b shows contour of dynamic pressure (in gauge scale) and it increases radially in quasi free vortex zone while in forced vortex zone it decreases. It reaches peak value at the interface between forced vortex and quasi-free vortex. The nature of dynamic pressure is asymmetric due to non-symmetry of tangential velocity.

Figure 5c shows the calculated tangential velocity distribution in detail. Tangential velocity and dynamic pressure distribution are quite similar in nature (reversing half part of tangential contour) which means tangential velocity can be considered as dominant velocity. The value of tangential velocity equals zero at the center of the flow field. It increases radially, reaches maximum and then decreases gradually. The ratio of maximum to minimum tangential velocity is more than 10. From Fig. 5d (B-B and C-C) it is clear that nature of axial velocity is same as that of tangential velocity. From the mathematics, it can be inferred that axial velocity is maximum where tangential velocity is minimum and vice versa, which is also satisfied by diagrams. The axial velocity has almost highest magnitude at the two opposite end of cyclone but opposite in direction at the upper section of barrel. In Fig. 5e (C-C) it can be noticed that the center of the forced vortex does not coincide with the geometrical center of cylindrical body, due to which it gets deflected to the gas inlet. This observation turned into eccentric vortex finder in some revised cyclone separators and proposal of some modification in inlet shapes has been reported by Suasnabar (2000). In Fig. 5e (A-A) Radial velocity is positive near the wall of conical section but it is negative at the center of conical section, which means particles are in the range of free vortex zone. Radial velocity is always positive in the free vortex zone of barrel section because there is no contact between particles and wall in this zone.

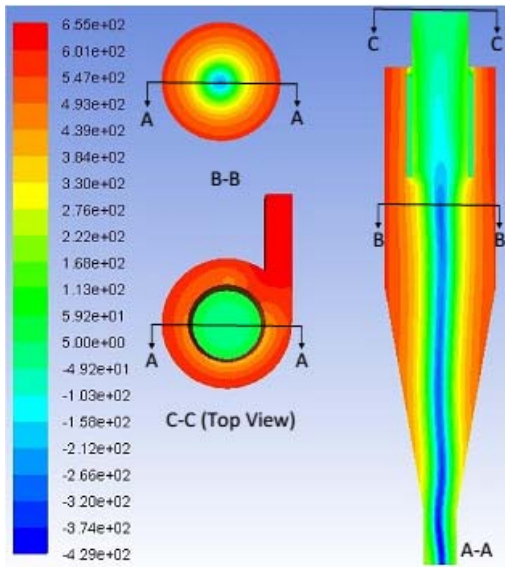


Fig. 5a. Contour of Static Pressure (Pa).

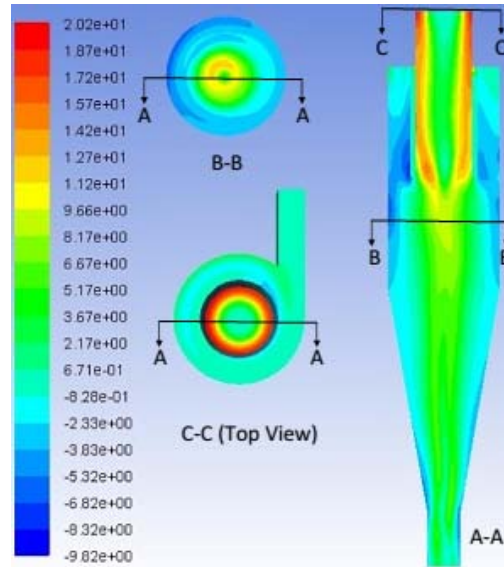


Fig. 5d. Contour of Axial Velocity (m/s).

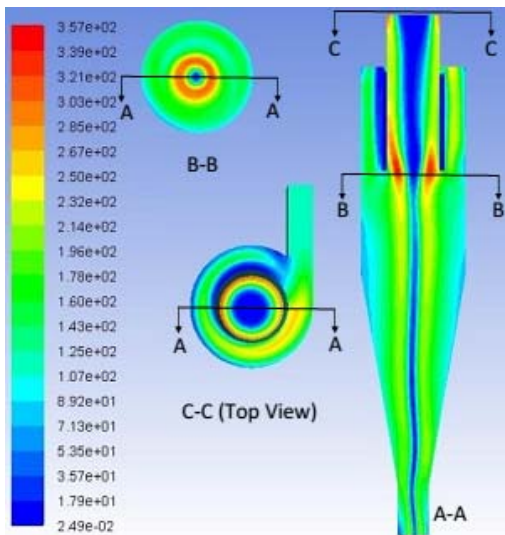


Fig. 5b. Contour of Dynamic Pressure (Pa).

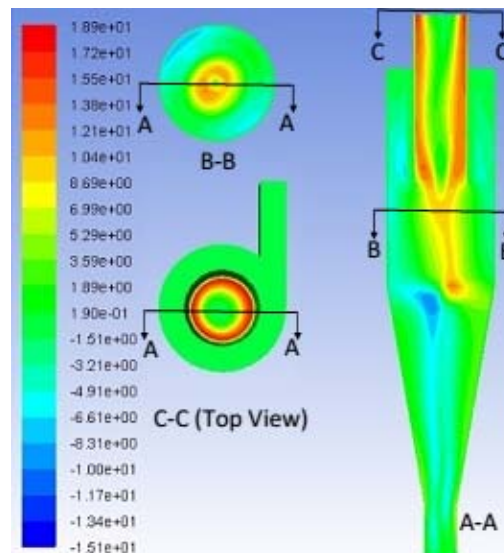


Fig. 5e. Contour of Radial Velocity (m/s).

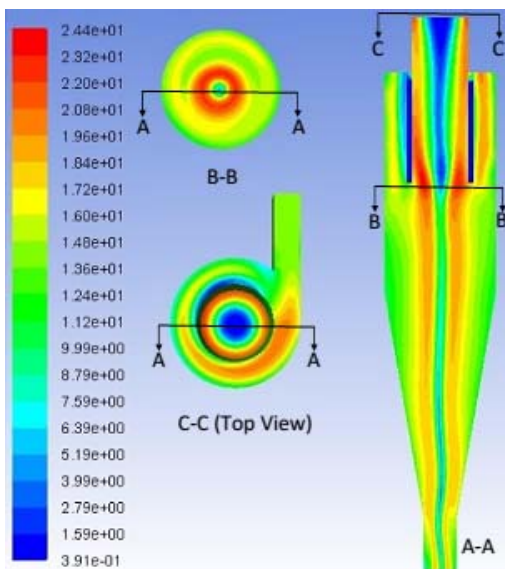


Fig. 5c. Contour of Tangential Velocity (m/s).

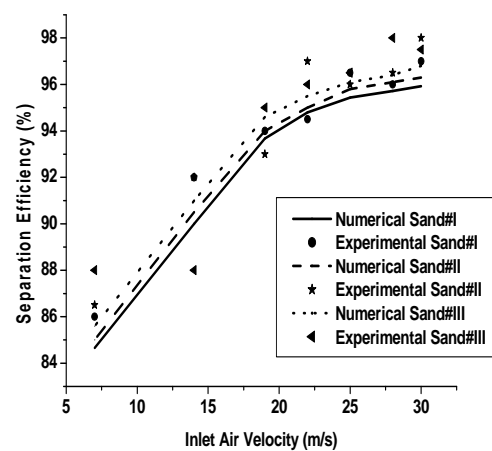
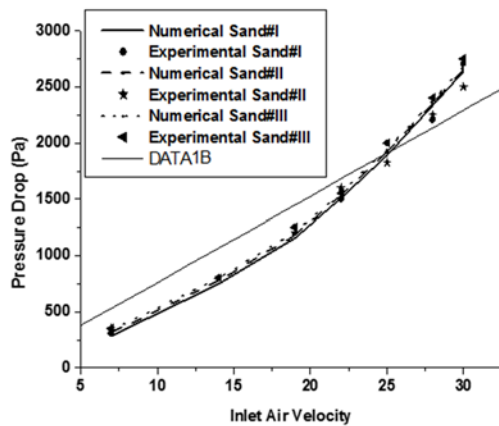


Fig. 6. Experimental results of separation efficiency compared with calculated results for three sand samples.



**Fig. 7. Experimental results of pressure drop compared with calculated results versus inlet air velocity for three sand samples.**

Figure 6. shows the experimental-numerical relation between separation efficiency and inlet air velocity for the three sand samples. Collection efficiency of cyclone is enhanced by increasing the inlet gas velocity. The curve is steep in the beginning (at low velocity) but gradually the slope becomes almost constant which means it has attained the maximum value. From the figure, it is clear that the numerical and experimental values match well. The variation in numerical value from the experimental one is between 0.29-2.17% for sand I, 0.21-2.06% for sand II and 0.41-3.41% for sand III.

For the three sand samples, pressure was measured across the two pressure taps and was found that pressure drop and inlet air velocity follows a potential growth pattern as shown in Fig. 7. The simulation results obtained for different inlet velocity matches well with the experiments conducted under similar conditions. The variation in numerical results from the experimental one is between 0.86-7.36% for sand I, 1.5-10.85% for sand II and 0.25-5.14% for sand III. The regression line shows a good fit of 0.9852 with an error of 4.6.

With the help of range of velocities for cyclone i.e., between 7m/s-30m/s, the superficial velocities for riser and loop seal was found to be 3.7-5.4 m/s and 0.14-0.85 respectively to run the CFB setup problem free.

## 6. CONCLUSIONS

Cyclone is an essential and cheap particulate separation process and is still being used globally in combustion and gasification processes. External circulating fluidized bed technology uses cyclone for trapping the solid particles and transfer to riser through standpipe. In the current paper, cold working of cyclone attached to CFB system has been studied in order to understand its stability in

the long run. On this basis, Reynolds stress model and discrete phase model has been used to predict the flow pattern of particles in the cyclone and is found to have good concord between the measured and calculated separation efficiency as well as pressure drop across the cyclone. The proposed model stipulates an expedient way to study the effects of variables related to operational conditions, particle size, coefficient of restitution and cyclone geometry.

It was found that best output was obtained at coefficient of restitution equal to 0.8, which is true for lab scale cyclone material i.e., 410 stainless steel having coefficient of restitution ranging from 0.7 to 0.8 for sand like particles. Separation efficiency of lab scale cyclone obtained from experiments ranges between 86% and 98% for velocity varying from 7m/s to 30 m/s for given sand samples and operating conditions. Optimum condition for supply of gas to the loop seal and riser was thus predicted by the research findings.

## REFERENCES

- Bhasker, C. (2010). Flow simulation in industrial cyclone separator. *Advances in Engineering software* 41, 220-228.
- Bloor, M. I. G. and D. B. Ingham (1957). The leakage effect in industrial cyclone. *Chem Eng Res Des* 53, 7-11.
- Bloor, M. I. G. and D. B. Ingham (1975). Turbulent spin in a cyclone. *Trans I chem. E* 53, 1-6.
- Boysan, F., W. H. Ayer and J. A. Swithenbank (1982). Fundamental mathematical-modeling approach to cyclone design. *Transaction of Institute Chemical Engineers*. 60, 222-230.
- Du, J. Y. and W. Tabakoff (1984). Numerical simulation of a dilute particulate flow over tube banks. *ASME Trans fluid Eng* 116, 770-7.
- Fraser, S.M., A. M. Abdel Razek and M. Z. Abdullah (2000). Computational and experimental investigations in a cyclone dust separator. *Proc Inst Mech Eng Part-E* 211, 241-57.
- Hamdy O., M. A. Bassily, H. M. El-Batsh and T. A. Mekhail. (2017). Numerical study of the effect of changing the cyclone cone length on the gas flow field. *Applied Mathematical Modelling* 46, 81-97.
- Hoekstra, A. J., J. J. Derksen and H. E. A. Van Den Akker (1999). An experimental and numerical study of turbulent swirling flow in gas cyclones. *Chemical Engineering Science* 54, 2055-2056.
- Houben, J. J. H., C. Weiss and E. Brunnmair. (2016). CFD Simulations of Pressure

- Drop and Velocity Field in a Cyclone Separator with Central Vortex Stabilization Rod. *Journal of Applied Fluid Mechanics* 9(1), 487-499.
- Jianren, F., S. Ping, C. Lihua and C. Kefa (1998). Numerical investigation of new protection method of the tube erosion by particle impingement. *Wear*. 223, 50-7.
- Kozołub, P., A. Klimanek, R. A. Białeccki and W. P. Adamczyk. (2016). Numerical simulation of a dense solid particle flow inside a cyclone separator using the hybrid Euler–Lagrange approach. *Particuology*, article in press.
- Leith, D. and D. Mehta (1973). Cyclone Performance and Design. Atmospheric Environment. Oxford: Pergamon Press 7, 527–549.
- Leung, A. Y. T. (2015). CFD simulation of cyclone separators to reduce air pollution. *Powder Technology* 286, 488-506.
- Pant, K., C. T. Crowe and P. Irving (2002). On the design of miniature cyclone for the collection of bioaerosols. *Powder Technology* 125, 260-265.
- Rafiee, S. E. and M. M. Sadeghiyazad. (2017). Efficiency evaluation of vortex tube cyclone separator. *Applied Thermal Engineering* 114, 300-327.
- Safikhani, H. and P. Mehrabian. (2016). Numerical study of flow field in new cyclone separators. *Advanced Powder Technology* 27, 379–387.
- Shun, R. and Z. Q. Li (2002). Simulation of strong swirling flow by use of different turbulence model. *Power Engineering* 22.
- Slack, M. D. (2000). Advances in cyclone modelling using unstructured grids. *Trans IChem*. 78, 1098-104.
- Sommerfeld, M. and C. H. Ho (2003). Numerical calculation of particle transport in turbulent wall bounded flows. *Powder Technology* 131, 1-6.
- Song, C., B. Pei, M. Jiang, B. Wang, D. Xu and Y. Chen. (2016). Numerical analysis of forces exerted on particles in cyclone separators. *Powder Technology* 294, 437-448.
- Song, J., Y. Wei, G. Sun and J. Chen (2017). Experimental and CFD study of particle deposition on the outer surface of vortex finder of a cyclone separator. *Chemical Engineering Journal* 309, 249-262.
- Suasnabar, D. J. (2000). Dense medium cyclone performance enhancement via computational modelling of the physical processes. Ph.D thesis.
- Talbi K., Z. Nemouchi, A. Donnot and N. Belghar. (2011). An Experimental Study and a Numerical Simulation of the Turbulent Flow under the Vortex Finder of a Cyclone Separator. *Journal of Applied Fluid Mechanics* 4 (1), 69-75.
- Wasilewski, M. (2017). Analysis of the effect of counter-cone location on cyclone separator efficiency. *Separation and Purification Technology*. Accepted manuscript.